

Efficiency calibration of the Ge(Li) detector of the BIPM for SIR-type ampoules

C. Michotte

Bureau international des poids et mesures, Pavillon de Breteuil, Sèvres.

Abstract – The absolute full-energy peak efficiency of the Ge(Li) γ -ray spectrometer has been measured between 50 keV and 2 MeV with a relative uncertainty around 1×10^{-2} and for ampoule-to-detector distances of 20 cm and 50 cm. All the corrections applied (self-attenuation, dead time, pile up, true coincidence summing) are discussed in detail.

1. Introduction

Within the framework of the SIR (Système international de référence; Rytz, 1983), participants are asked to check the purity of their solution before submission. Verification of impurities is essential at the BIPM in the case of discrepant results or for short-lived radionuclides (Michotte, 1999). This can be achieved using a γ -ray spectrometer for fast standardizations and purity checks, which are also very useful in the daily work of the Ionizing Radiation section.

For these reasons, it was decided to develop a γ -ray spectrometer at the BIPM. Ideally, the purity check of an SIR ampoule should be made in a non-destructive way, i.e. without opening it. Therefore, the detector has been calibrated in efficiency directly for SIR-type ampoules. The detector can also be calibrated subsequently for point sources if needed for other applications. In this report, the efficiency calibration of the Ge(Li) detector available at the BIPM is presented. This detector has been used to develop and test the method of measurement. It will be replaced in the near future by an HPGe which has better characteristics and is more sensitive to the detection of impurities.

In this report, the term "efficiency" is used to mean the absolute full-energy peak efficiency, i.e. the ratio of the counts in the full-energy peak to the number of the corresponding γ -rays emitted by the source.

2. Detection setup

The Ge(Li) detector is a closed-end coaxial crystal with a nominal active volume of 60 cm^3 , mounted in an aluminium outer cap. It is connected to a resistive feedback preamplifier. The detection geometry is presented in Figure 1. The 5 cm-thick lead shielding and the Pb-x ray absorber in cadmium reduce the background level in the whole energy range (from 30 keV to 2 MeV) to about 2 counts per second. The ampoules may be positioned at 20 cm or 50 cm from the detector. Two lucite holders are available: one is 1 mm thick and the other is 9.4 mm thick around the ampoule in order to stop high-energy β particles emitted by sources like ^{56}Co , as they would distort the γ -ray spectra by producing β - γ coincidences. As lucite is composed of low-Z elements, no additional bremsstrahlung has been observed in the Ge(Li) spectra above 30 keV. The resolution remains unchanged when using the thick holder,

but the peak-to-Compton ratio is slightly reduced. For a given ampoule the relative repeatability of its positioning in the holder is estimated by measurement to be better than 1.5×10^{-3} .

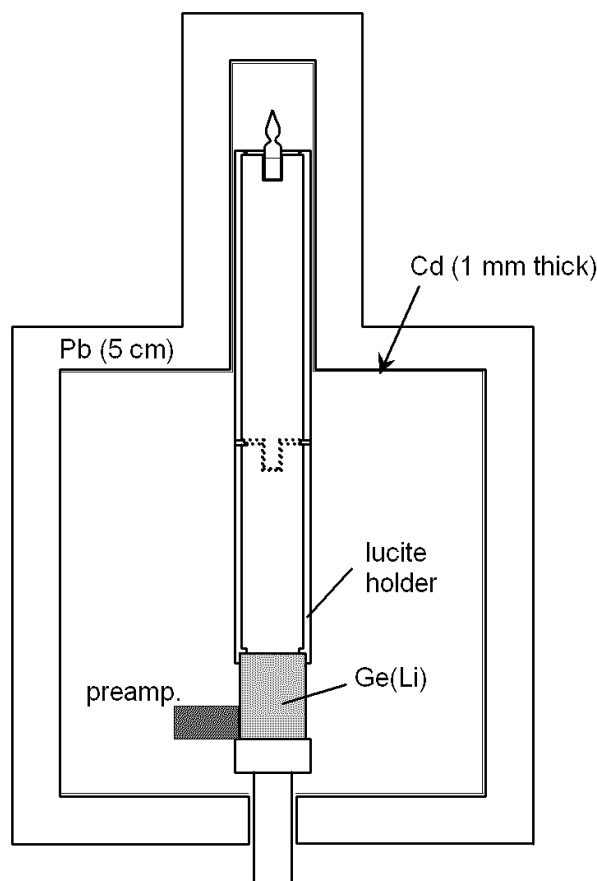


Figure 1: Geometry of the gamma-ray spectrometer at the BIPM.

2.1. Uncertainties related to the use of extended sources

Small differences in shape and thickness of the SIR-type ampoule base were observed by Rytz (1983), although the ampoules were (and still are) from the original batch. This generates variations in the ampoule position which are negligible when compared to the large source-to-detector (D) distance. On the other hand, it produces measurable changes in the attenuation of the γ -ray flux by the glass, especially at low γ -ray energy. The uncertainty of activity measurements arising from these variations has been evaluated experimentally using empty ampoules which were cut in two parts, and by placing the glass base between a point source and the detector. Repeatability of measurements of a single ampoule is within the statistical uncertainties. Relative standard uncertainties of 2×10^{-3} at 1.2 MeV and 4.5×10^{-3} at 60 keV were derived (see Figure 2).

Other sources of uncertainty are the volume and density of the radioactive solution, which may vary between the ampoules. To account for this, a correction factor is evaluated -

assuming a distant source-detector geometry and exploiting the cylindrical symmetry - using the density ρ and the mass m of the solution quoted on the SIR form by the national laboratory which is asked to fill the ampoule with around 3.6 g of radioactive solution:

- Fluctuations in the solid angle Ω due to variations of the filling height h of the ampoules are estimated from the expression

$$\frac{\Delta\Omega}{\Omega} = \frac{\Delta h}{D + h} ,$$

where

$$h = \frac{m}{\rho S} = \frac{\mu}{\rho} ,$$

S is the nominal section of the SIR-type ampoules (1.8 cm²) and $\Delta h = (h - 2)$ cm. These relative fluctuations are lower than 3×10^{-3} .

- Changes in μ , the height of the solution measured in mass per unit area, produce variations in the attenuation of the γ rays that can be corrected by the factor

$$C_{\mu} = 1 + \frac{\Delta\mu}{\mu} - \frac{\Delta\mu}{\lambda(e^{\mu/\lambda} - 1)}$$

where $\Delta\mu = (\mu - 2)$ g/cm² and λ is the photon mass attenuation length (mean free path) in water at the energy considered (Debertin and Helmer, 1988). The factor C_{μ} is obtained assuming a constant solid angle over the ampoule height. In most cases, this correction factor is lower than 5×10^{-3} in relative terms. However, it may reach 15×10^{-3} for low-energy γ -ray emitters in a high-density solution.

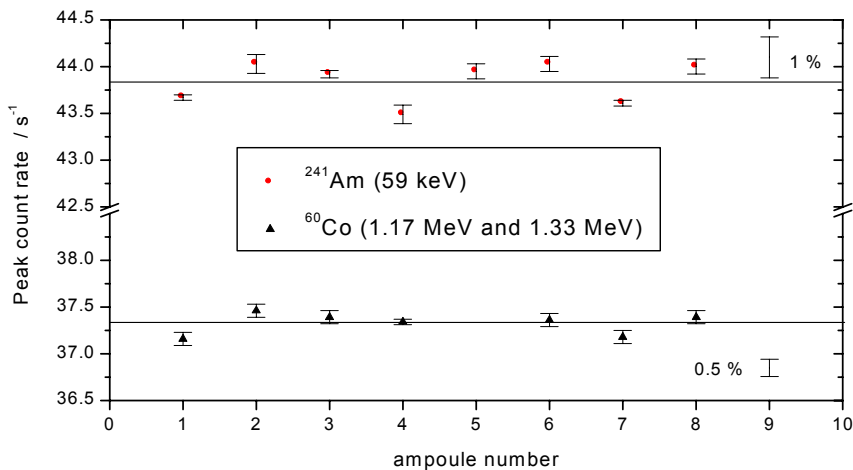


Figure 2: Fluctuations of full-energy peak count rates corresponding to changes in the glass ampoule base placed between a point source and the Ge(Li) detector.

3. Electronics

3.1. Block diagram of the electronics

The block diagram of the electronics is presented in Figure 3a. It ensures that dead-time and pile-up corrections are independent of the analogue-to-digital converter (ADC) and of the multichannel analyzer. Indeed, these corrections are determined by the sequence of electronic modules consisting of the low-level discriminator¹ followed by a dead-time module which generates a gate signal G to control the digital conversion of the linear unipolar pulses arriving at the Linear-Gate-and-Stretcher module (LGS). The dead-time module is identical to those used extensively in connection with $4\pi\beta\text{-}\gamma$ coincidence methods. The module was developed at the BIPM and calibrated by the two-oscillator method (Bréonce, 1981). It inserts a non-extended dead time by impeding the transmission of logic signals during the time chosen. The latter is sufficiently long ($51\ \mu\text{s}$) to allow a complete conversion of the linear pulse before accepting another event. The dead-time correction is evaluated afterwards using the known formula for non-extended dead time (see section 5.1).

When a gate signal is present, the LGS converts the unipolar pulses from the amplifier into linear square pulses which are then analysed by a Wilkinson/100 MHz CANBERRA ADC (set in the non-overlap mode). This ensures that only the pulses above the discrimination level L_D are processed by the ADC. There is a significant advantage in gating the LGS as opposed to the ADC²; in the absence of a gate signal G the LGS does not process any input linear pulse at all and, in consequence, does not generate the dead time which would have not been taken into account by the dead-time correction. The timing diagram of the electronics is shown in Figure 3b.

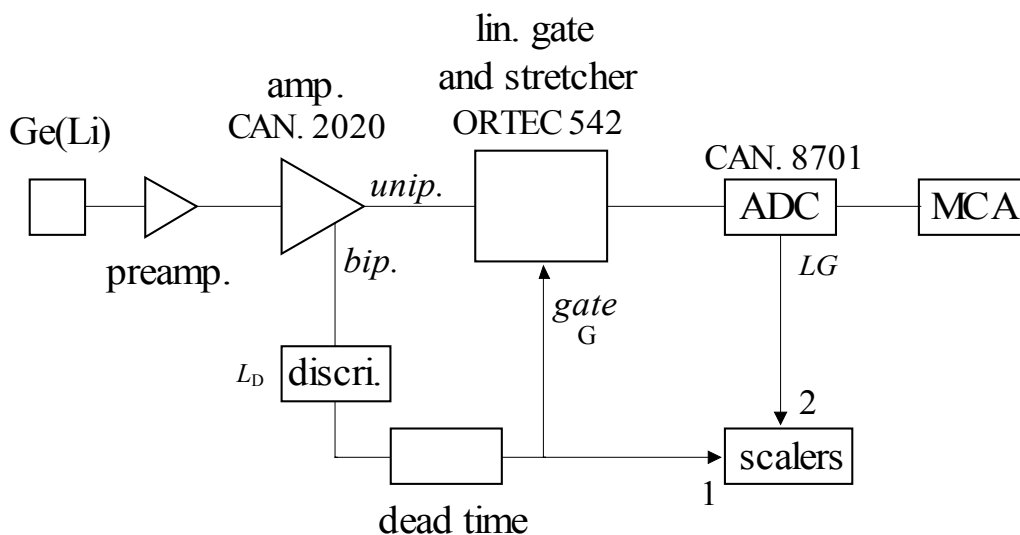


Figure 3a: Block diagram of the electronics connected to the Ge(Li) detector. The signal LG indicates that the ADC has detected a pulse from the LGS.

¹ The internal lower thresholds of the ADC and the LGS must be set below the discrimination level L_D

² In a first attempt, no LGS was used and the signal G was used to gate the ADC directly. In this case, all unipolar pulses arrive at the ADC and it was observed that these pulses produce some dead time in the ADC even in the absence of a gate signal. This dead time is not taken into account in the dead-time correction.

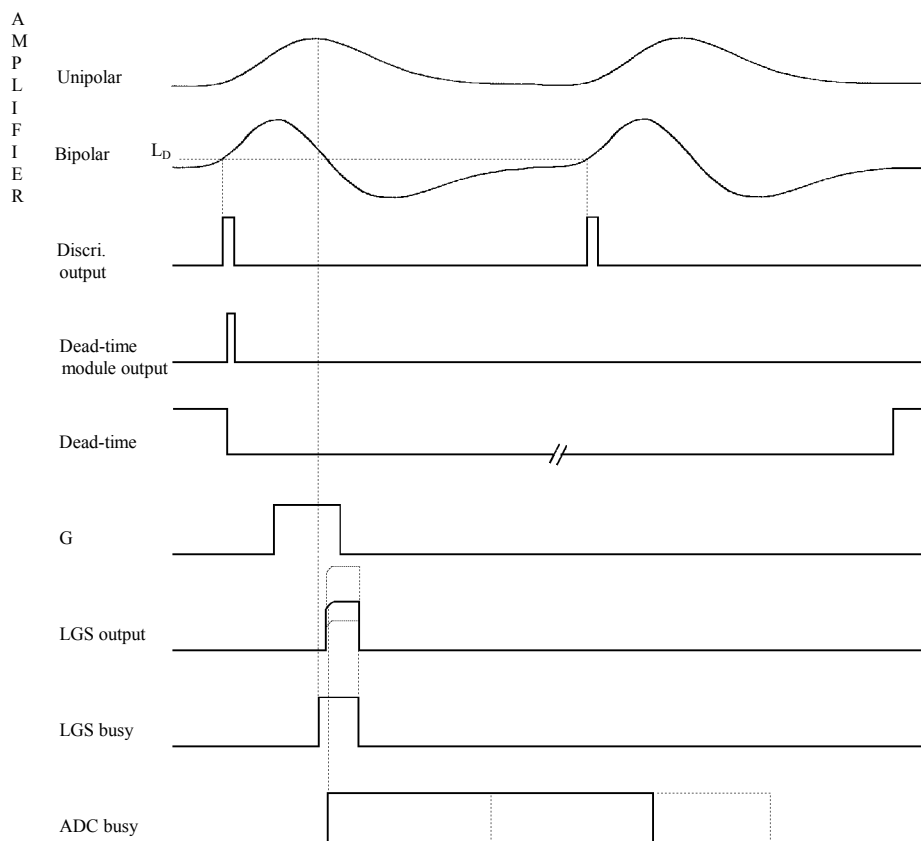


Figure 3b: Timing diagram of the electronics connected to the Ge(Li) detector.

3.2. Characteristics of the system

The resolution (FWHM) of the Ge(Li) detector is 2.3 keV at 1.33 MeV. The full widths at 1/10th and 1/50th of the maximum height are equal to 2.0 x FWHM and to 3.3 x FWHM, respectively. The relative loss in energy resolution due to the use of the LGS is only 4 %. These poor characteristics justified the purchase of the HPGe detector mentioned in the Introduction.

The stability of the electronics is satisfactory as the typical relative gain drift, observed after several days of measurement, is only 4×10^{-4} .

4. Peak integration method

Fitting the highly asymmetrical full-energy peaks from the Ge(Li) spectrometer is not trivial and many parameters are involved (e.g. two low-energy tails are needed to simulate more closely the shape of the peaks). In consequence, it was preferred to evaluate the peak area by simple summation of the channel contents in an interval around the peak, having a width of 7.5 times the FWHM of the peak. The continuum under the peak is assumed to be linear and determined from the summation of counts in intervals having a width of 3 x

FWHM on both sides of the peak. When the continuum is clearly non-linear, the limits of the summation intervals are modified and reduced to the minimum acceptable. In the case of two closely spaced peaks, both are integrated together.

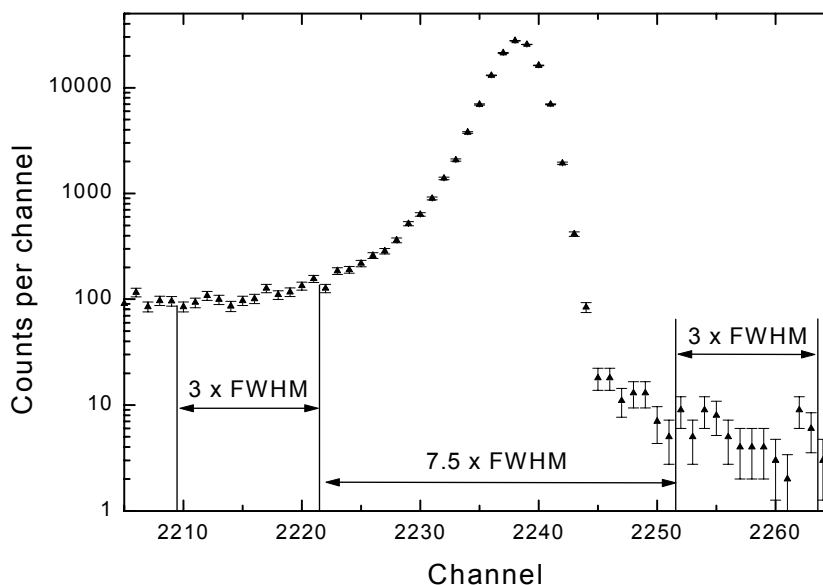


Figure 4: ^{60}Co γ -ray energy spectrum: 1.33 MeV full-energy peak and the channel intervals used for its integration. FWHM = 2.34 keV. Total count rate = 450 s^{-1} .

5. Correction factors

5.1. Dead-time correction

The dead-time correction factor is $(1 - R\tau)^{-1}$, where τ is the dead-time value selected for the dead-time module and R is the total count rate above the threshold including the digital overflows (pulses exceeding the ADC range), as given by the scaler no. 2 shown in Figure 3a. This rate has been checked and is exactly equal to the rate of the gate signals G , given by the scaler no.1. To test the method, the same ^{60}Co energy spectrum has been measured for several values of τ . The count rate $R_{\text{ROI,c}}$ in the region of interest around the full-energy peaks, corrected for dead time, is plotted versus τ in Figure 5. Above $\tau \cong 40\ \mu\text{s}$, $R_{\text{ROI,c}}$ remains constant within the uncertainties, showing that the overall dead time of the electronics behaves as non-extended and that the method described is consistent. For low τ values, $R_{\text{ROI,c}}$ drops rapidly because τ becomes shorter than the dead time of the ADC which, in consequence, induces additional losses not taken into account by the correction factor.

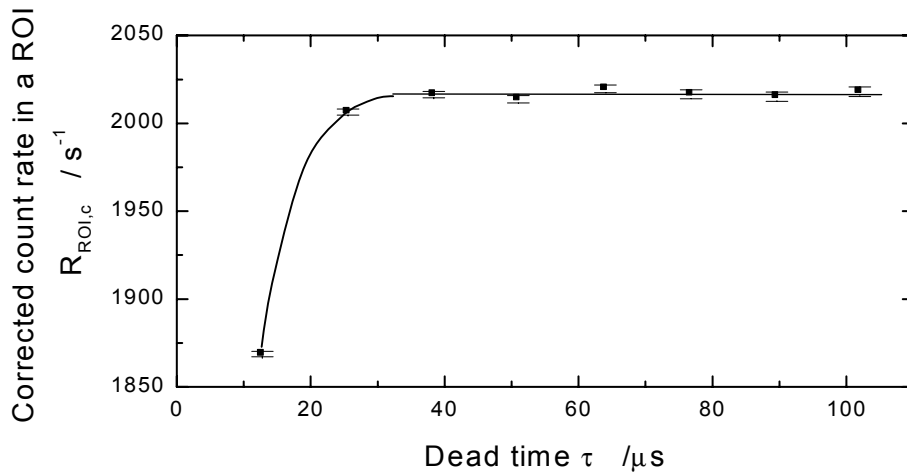


Figure 5: Count rate in the region of interest (ROI) around the ^{60}Co full-energy peaks, corrected for dead time, versus the dead time selected for the dead-time module. The total count rate in the energy spectrum ranges from 6×10^3 ($\tau = 102 \mu\text{s}$) to 12×10^3 ($\tau = 13 \mu\text{s}$) counts per second.

5.2. Pile-up correction

As no measurements are intended to be made at high count rates, electronic circuits for pile-up rejection have not been used. The pile-up correction factor was measured using the two-source method, i.e. by using an additional source near the detector to increase the count rate and thus induce pile up (e.g. Debertin and Helmer, 1988). The area of a full-energy peak of a γ ray emitted by the source placed in the lucite holder is then plotted versus the total count rate corrected for dead time, i.e. $R_c = R(1 - R\tau)^{-1}$, which is a function of the distance to the detector of the second source. The data are fitted by a linear function and normalized by dividing by the extrapolated value at zero count rate. Some results are shown in Figure 6a. Figure 6b is another presentation of the results: the gradient of the linear fit is plotted versus the energy of the peak considered. The radionuclide used as a second source is indicated. The measurements made for ^{60}Co show that the lower the γ -ray energy of the second source, the higher is the absolute value of the gradient. This is an unwanted effect as the pile-up correction should not depend on the radionuclide used to increase the count rate.

Figures 7a and 7b illustrate that the distortion shown in Figure 6b no longer occurs if the count rate R_0 below the discrimination level is taken into account. For each measurement, R_0 is obtained by extrapolating the energy spectrum to zero energy and integrating it from zero to the threshold around 25 keV. This extrapolation has been carried out using several functions. An uncertainty of type B on R_0 is then estimated from the difference between the various results obtained. The two-source method is limited experimentally by the requirement that the γ rays from the second source must have an energy lower than one half that of the γ rays of the first source. Thus the pile-up correction could not be measured for low energies and had to be extrapolated from higher energies. In consequence, the relative uncertainty of this correction reaches 6×10^{-3} below 100 keV for a count rate lower than 1500 s^{-1} and it increases rapidly with the count rate.

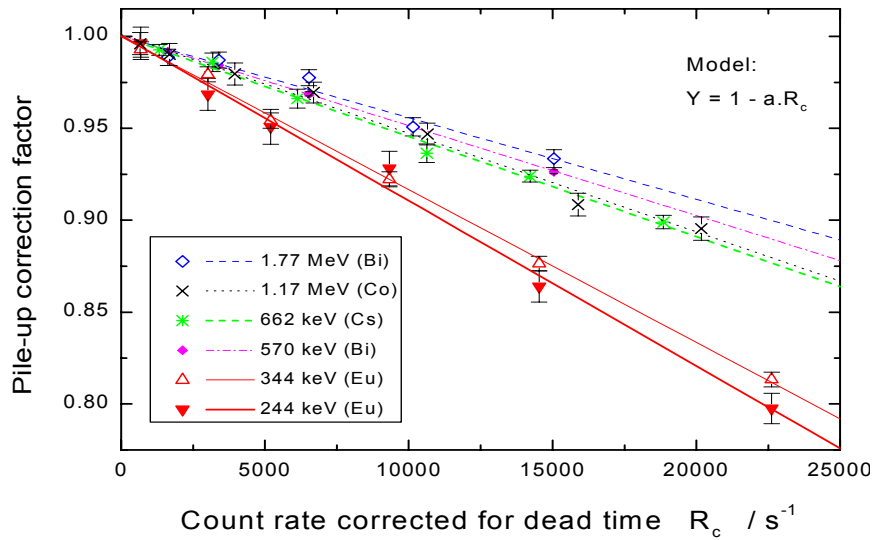


Figure 6a: Measured pile-up correction factor versus the count rate above the threshold, corrected for dead time. The straight lines are linear fits.

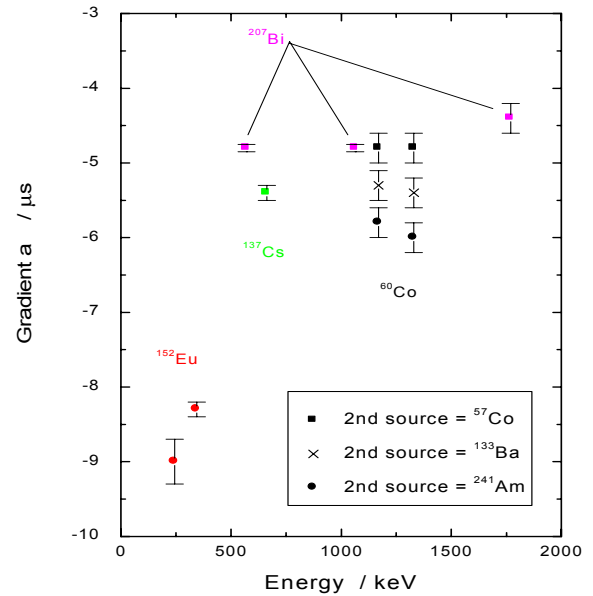


Figure 6b: Gradient of the linear fits of Figure 6a, versus the gamma-ray energy. The radionuclide used to increase the count rate is indicated.

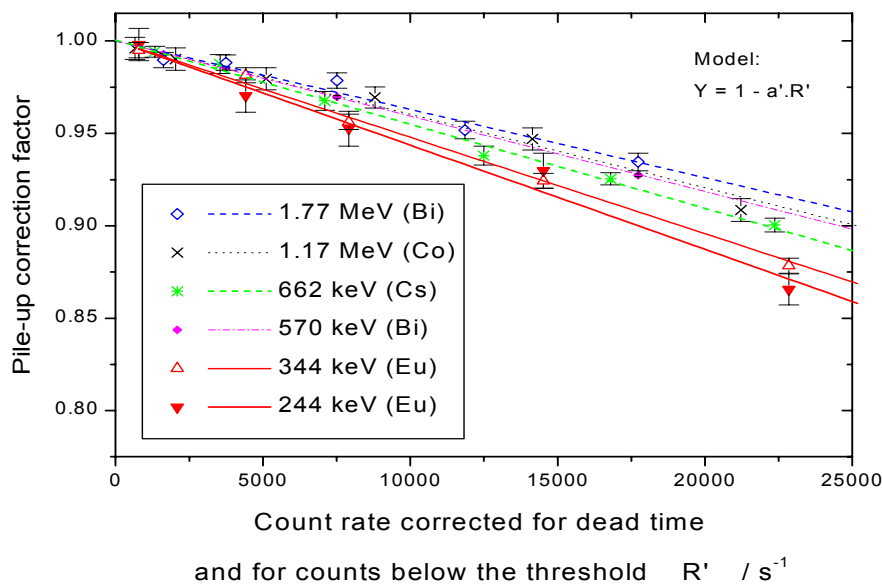


Figure 7a: Similar to Figure 6a, but the count rate below the threshold has been taken into account.

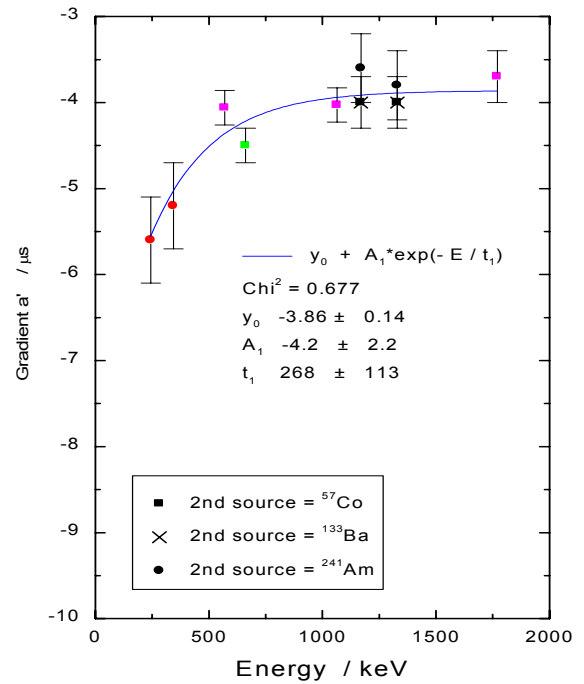


Figure 7b: Gradient of the linear fits of Figure 7a, versus the gamma-ray energy E . The radionuclide used to increase the count rate is indicated.

5.3. True coincidence summing

The true coincidence summing (TCS), which occurs when several γ rays are emitted in cascade is evaluated by the KORSUM FORTRAN program developed at the PTB, considering the SIR ampoules as point sources. KORSUM does not take into account coincidence summing between γ and β rays, and neglects the possible angular correlation between the cascading γ rays (e.g. Debertin and Helmer, 1988). To run this program, the total efficiency of the spectrometer versus the γ -ray energy is needed and has been measured using SIR ampoules of (quasi-)single γ emitters. Each energy spectrum has been extrapolated to zero energy to obtain the total count rate in the detector. No pile-up correction is applied as it should be in integral measurements. The results for $D = 20$ cm are presented in Figure 8. The two lowest data points (at around 35 keV) correspond to x-ray measurements for which the total efficiency is obtained by integrating the x-ray peaks. A pile-up correction is then needed as for gamma full-energy peak efficiencies.

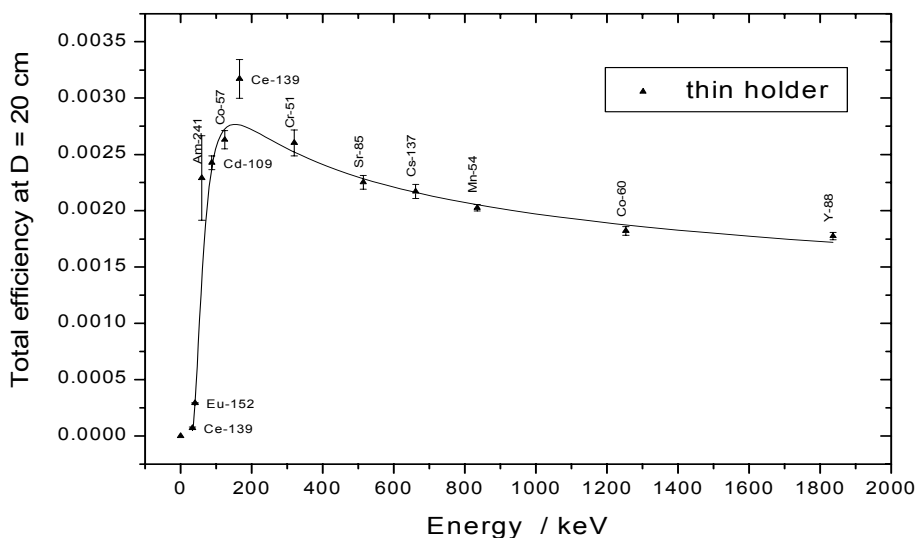


Figure 8: Total efficiency of the Ge(Li) spectrometer measured using SIR ampoules from eight different NMIs. KORSUM showed that the TCS correction is significant only for the short D distance (20 cm) where it can reach as much as 6×10^{-3} in rare cases, for example with ^{56}Co . Tests have

indicated that the TCS correction shows little sensitivity to 10 % fluctuations in the efficiency curves used as input data by the program (see Table 1).

Radionuclide	γ -ray energy / keV	TCS correction (KORSUM) for D = 20 cm	
		Total efficiency from Fig. 8	Earlier values of tot. eff.
²² Na	1275	1.004	1.004
⁵⁶ Co	847	1.004	1.003
	977	1.006	1.006
	1038	1.005	1.005
	1238	1.005	1.005
	1771	1.004	1.004
⁶⁰ Co	1173	1.002	1.002
	1333	1.002	1.002
¹³³ Ba	53	1.003	1.003
	81	1.003	1.003
	223	1.002	1.002
	276	1.002	1.002
	303	1.001	1.001
	356	1.001	1.001
¹⁵² Eu	122	1.003	1.003
	245	1.004	1.004
	411	1.004	1.004
	444	1.003	1.003
	779	1.002	1.002
	964	1.002	1.002
	1112	1.001	1.002
	1408	1.002	1.002
¹⁶⁹ Yb	94	1.005	1.005
	131	1.004	1.004
	177	1.003	1.003
	198	1.003	1.003
	261	0.99	0.99
	308	0.998	0.998
¹⁹² Ir	205	1.004	1.003
	468	1.003	1.003

Table 1. TCS correction factors calculated with the KORSUM program and using either the total efficiency curve shown in Figure 8 (col. 3) or earlier values which differ by up to 10 % (col. 4).

6. Efficiency measurements

As far as possible, ampoules that gave an equivalent activity in good agreement with the international mean value were selected for the calibration. In addition, to minimize the uncertainties, only well-known and isolated gamma lines are considered. Each measurement was repeated at least twice. For short-lived radionuclides the measurement duration was limited to some hundreds of seconds in order to have a constant count rate, as required for the present dead-time and pile-up corrections. A typical uncertainty budget of an efficiency measurement of the Ge(Li) detector is given in Table 2.

	Relative uncert.	Comment
Dead time	$< 3 \times 10^{-4}$	for count rates $< 5000 \text{ s}^{-1}$
Pile up	$(3 \text{ to } 6) \times 10^{-3}$	for count rates $< 1500 \text{ s}^{-1}$
True coincident summing	1×10^{-3}	if relevant
Self attenuation of the solution	1×10^{-3}	
Atten. by the ampoule base	$(1 \text{ to } 5) \times 10^{-3}$	depending on gamma-ray energy
Ampoule position	1×10^{-3}	
Ampoule activity	$(1 \text{ to } 10) \times 10^{-3}$	as given by the NMI
Decay correction, γ emission probability	$< 15 \times 10^{-3}$	using nuclides having a decay scheme with small uncertainties

Table 2. Uncertainty budget of an efficiency measurement with the Ge(Li) detector.

The logarithm of the measured full-energy peak efficiency is plotted against the logarithm of the γ -ray energy. The data are split into a low-energy and a high-energy group with a large overlap (from 155 keV to 550 keV) and fitted to a 3rd and 4th order polynomial, respectively. The overlap is sufficiently wide to ensure a common fitted curve for the two groups of data, allowing a smooth transition from one polynomial to the other at around 310 keV. The resulting efficiency curves and residuals are shown in Figures 9a-b. The smooth line on each plot of the residuals corresponds to the relative uncertainty of the fit of the efficiency data. However, other fits of the data may be made, giving slightly different curves. It was observed that the uncertainty of the fit does not reflect these differences, especially around 200 keV. It was then decided to evaluate the total uncertainty of the efficiency curves from the distribution of the residuals (Debertin and Helmer, 1988). This is shown on the same figures as the residuals, by the stepped lines.

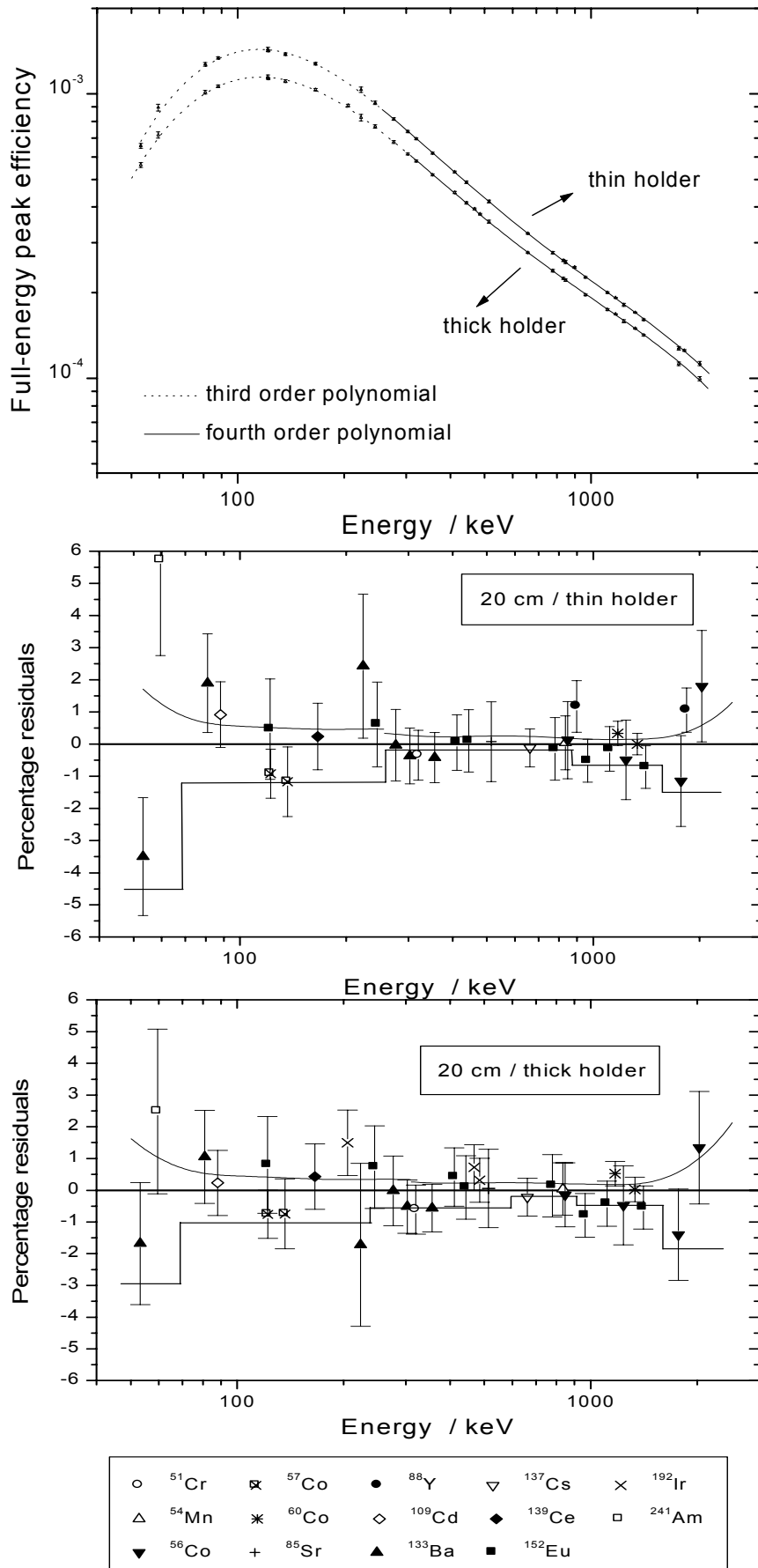


Figure 9a: Efficiency of the Ge(Li) spectrometer for $D = 20$ cm, using the thin and thick lucite holder, and the percentage residuals (see text).

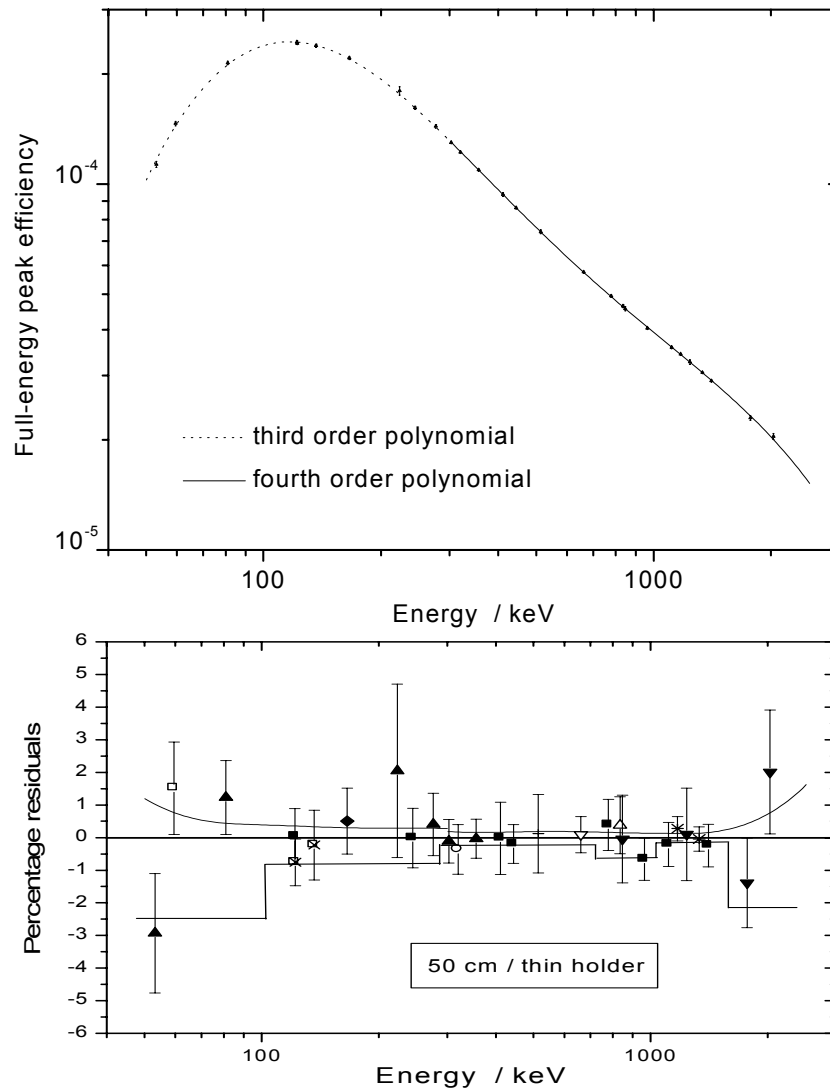


Figure 9b: Efficiency of the Ge(Li) spectrometer for $D = 50$ cm using the thin lucite holder, and the percentage residuals (see text). The legend is the same as in figure 9a.

The comparison of the residuals obtained with a thin and a thick lucite holder for the ampoules does not show any evidence of the influence of β - γ coincidences. This needs to be checked again for the HPGe which has a thin Be window and so could be more sensitive to these coincidences.

The long-term stability of the detector is monitored by periodic measurements of ^{137}Cs and ^{60}Co ampoules. A decreasing trend in the efficiency is observed for both ampoules, but with a different gradient (see Figure 10). This increases the uncertainty of further measurements with the Ge(Li) spectrometer which needs, in consequence, to be replaced by the HPGe detector as soon as possible.

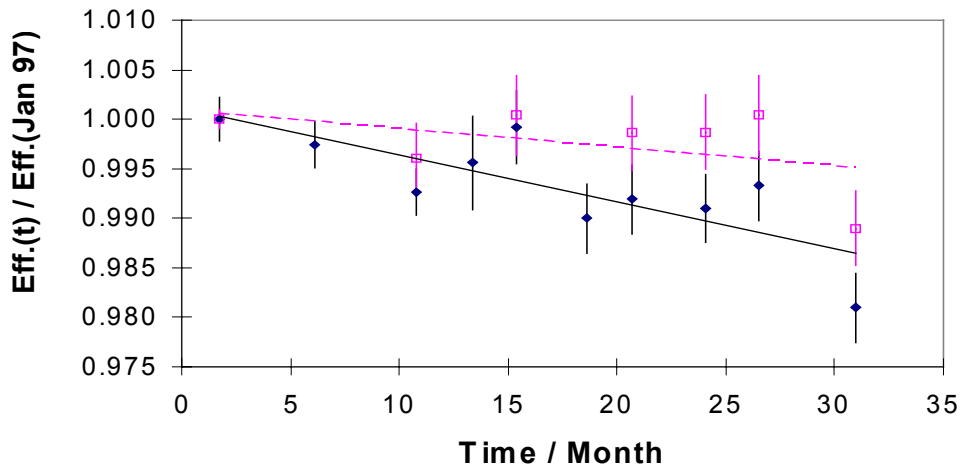


Figure 10: Long-term stability of the Ge(Li) spectrometer. The open squares are ^{137}Cs measurements and the diamonds ^{60}Co measurements. Correlated uncertainties have been subtracted. The dashed and straight lines are linear fits of the ^{137}Cs and ^{60}Co data, respectively.

7. Test measurements

To test the accuracy of the present calibration, several SIR ampoules were measured and the results compared with those given by the participating NMI (see Figure 11). All the BIPM Ge(Li) measurements are in agreement to within 1 or 2 standard uncertainties with the NMI values.

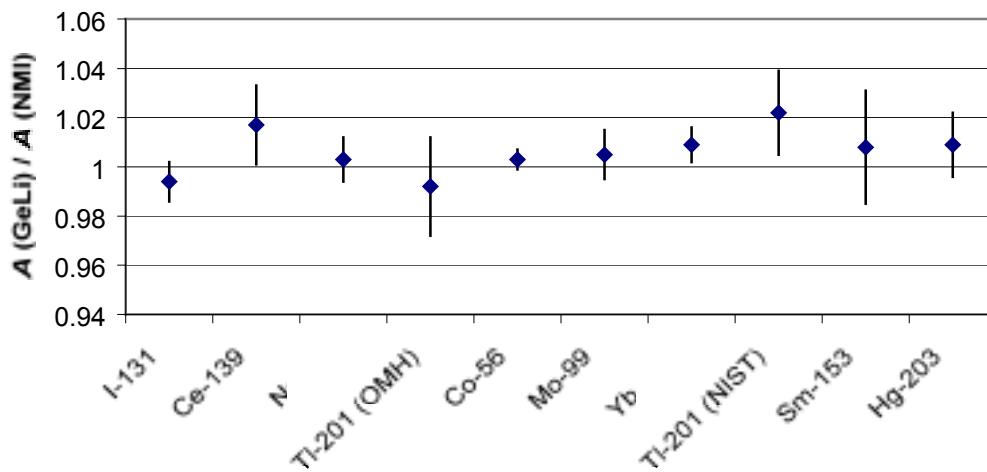


Figure 11 : Activity measured with the Ge(Li) compared to the value given by the NMI which standardized the SIR ampoule. The former activity is the weighted mean of the values obtained for several γ -rays. The plotted uncertainties are the quadratic sum of the standard uncertainties of the Ge(Li) and NMI measurements.

8. Conclusion

The electronics of the Ge(Li) spectrometer at the BIPM have been assembled and tested extensively. The dead-time and pile-up corrections to be applied to the data have been determined and are reported here. Each spectrum is extrapolated to zero energy to obtain the total count rate, including the counts below the threshold, which is needed for the pile-up correction. The true coincidence summing correction, which is in the range of 10^{-3} , was evaluated with KORSUM from the PTB. The calibrations were performed at two distances from the detector. The results were less precise at the shorter distance where the count rate is generally higher and the measurement is more sensitive to the pile-up correction. The effect of using SIR ampoules instead of point sources to calibrate the detector has been studied in detail. It limits the precision of the present calibration only below 100 keV. The relative standard uncertainty of the efficiency curves is less than 1×10^{-2} across almost all the energy range. The Ge(Li) has been tested in two EUROMET exercises and gave results in agreement with the other participants within the uncertainties. The spectrometer is now used for the search of radioactive impurities in SIR ampoules, and has produced useful results in the case of short-lived radionuclides (Michotte et al., 1999 and Michotte, 1999). However, the characteristics of the Ge(Li) detector seem to deteriorate slowly and efforts will be concentrated on the calibration of the HPGe detector which is now available at the BIPM.

Acknowledgement - The author wishes to thank M. Nonis for technical support, Drs K. Debertin and U. Schoetzig for discussions about KORSUM and Drs G. Ratel, J.W. Müller, P.W. Martin, J. Morel, M. Etcheverry, M.-C. Lépy, P. De Felice, M. Décombaz, J.-J. Gostely, S.A. Woods and J. Vanhorenbeeck for discussions about dead time, pile up,... and general discussions about gamma spectrometry.

References

- Bréonce, P., 1981. *Description d'un dispositif automatique de mesure précise de temps morts*. Rapport BIPM-81/1, Sèvres, France.
- Debertin, K. and Helmer, R.G., 1988. *Gamma- and x-ray Spectrometry with Semiconductor Detectors*. North-Holland, pp. 258-281.
- Michotte C. et al., 1999. *First measurement of ^{153}Sm in the SIR*. Rapport BIPM-99/9.
- Michotte C., 1999. *Influence of radioactive impurities on the SIR measurements*. ICRM'99 contribution, Prague. Accepted for publication in Appl. Rad. Isot.
- Rytz, A., 1983. *The international reference system for activity measurements of γ -ray emitting nuclides*. Appl. Rad. Isot. 34 (8), 1047-1056.